ELSEVIER

Available online at www.sciencedirect.com
SCIENCE DIRECT

Microelectronic Engineering 69 (2003) 190–194

MICROELECTRONIC ENGINEERING

www.elsevier.com/locate/mee

Oxygen vacancy defects in tantalum pentoxide: a density functional study

R. Ramprasad[a,*], Michael Sadd[b], Doug Roberts[b], Tom Remmel[a], Mark Raymond[b], Eric Luckowski[b], Sriram Kalpat[b], Carole Barron[b], Mel Miller[a]

[a]*Motorola Semiconductor Products Sector, 2100 E. Elliot Road, Tempe, AZ 85284, USA*

[b]*Motorola Semiconductor Products Sector, 3501 Ed Bluestein Blvd, Austin, TX 78721, USA*

Abstract

First principles total energy calculations were performed in order to characterize O vacancy defects in Ta_2O_5. A simplified version of the crystalline orthorhombic phase of Ta_2O_5 was used in this study. Results indicate that O vacancies in Ta_2O_5 can be broadly classified based on their location in the lattice. One type of vacancy (occupying the 'in-plane' sites) displays deep or mid gap occupied states, and shallow unoccupied states, while a second type (occupying 'cap' sites) results in shallow occupied states. For a wide range of local Fermi level or chemical potential, the neutral and +2 charged states of the in-plane type vacancy and the +2 charge state of the cap type vacancy are found to be most stable.

© 2003 Elsevier B.V. All rights reserved.

Keywords: Defect states; Trap states; Tantalum pentoxide; Oxygen vacancy; Density functional theory

1. Introduction

Although tantalum pentoxide (Ta_2O_5) has been studied both experimentally and theoretically over the past three decades, its real emergence as a dielectric material that can be integrated with conventional CMOS has happened only in the last decade [1]. While interest in high dielectric constant materials in general is primarily due to a need to scale down device sizes, the renewed interest in Ta_2O_5 is due to the ability to deposit it using conventional methods compatible with equipment and processes already available in the semiconductor industry. Nevertheless, concerns exist with Ta_2O_5 (and other alternative dielectric materials), one of them being defect densities, and their impact on the leakage currents (via defect or 'trap' levels created in the band gap of the dielectric).

The present work attempts to theoretically characterize oxygen vacancy defects in Ta_2O_5. The atomistic structure of Ta_2O_5 was chosen so that it is computationally tractable, while at the same time is representative of deposited films. Different types of O vacancies with qualitatively different types of coordination environments were considered within this model, and the defect or 'trap' levels due to these defects were determined using first principle total energy calculations. Correlations between the coordination environment and the location of the defect levels were identified. The stability of variously charged vacancies was also considered as a function of the vacancy type and the local chemical potential.

This paper is organized as follows. In Section 2, we provide details of the calculation methods and the

*Corresponding author.
E-mail address: r.ramprasad@motorola.com (R. Ramprasad).

0167-9317/03/$ – see front matter © 2003 Elsevier B.V. All rights reserved.
doi:10.1016/S0167-9317(03)00296-X

atomistic model of Ta_2O_5 used in this work. Section 3 discusses the results: structural aspects of the local coordination environment of Ta ions in Ta_2O_5 are compared with measurements in Section 3.1, the location of O vacancy induced defect levels in the band gap of Ta_2O_5 is discussed in Section 3.2, and the relative stability of charged O vacancies is presented in Section 3.3. We finally conclude with Section 4.

2. Model and method

Crystalline Ta_2O_5 occurs in several different polymorphs, with the orthorhombic phase containing 11 formula units (22 Ta and 55 O atoms) being the most stable [2]. The building blocks of the orthorhombic structure are TaO_6 (octahedral) and TaO_7 (pentagonal bipyramidal) polyhedra [2]. In the present work, for computational ease, a simplified version of the actual orthorhombic unit cell containing two Ta_2O_5 formula units (4 Ta and 10 O atoms) and two TaO_6 and two TaO_7 polyhedra were used (Fig. 1). Although the chosen model of Ta_2O_5 is crystalline, it will be shown in the next section that the local environment of Ta and O in this model is consistent with that of fabricated Ta_2O_5 films.

All calculations were performed using the local density approximation (LDA) with in density functional theory (DFT), as implemented in the Vienna ab initio simulation package (VASP) [3], using ultrasoft pseudopotentials. A plane-wave basis set with an energy cutoff of 29 Ry for the wave function and 68 Ry for the electron density was used. Defect free bulk Ta_2O_5 calculations were performed with 12 k points in the irreducible wedge of the Brillouin zone (IBZ); increasing the number of k points was found to have negligible effects on both the structure and the total energy. O vacancy calculations were performed with twice the size of the bulk unit cell (containing 8 Ta and 19 O atoms), and 8 k points in the IBZ. Further doubling the size of the unit cell for the O vacancy calculation had negligible effects on the vacancy formation energy for neutral as well as charged vacancy calculations. All calculations involved relaxation of the atomic positions until the forces on each atom were below 0.04 eV/A.

Defect state energies were calculated using total energy results of separate +1 and −1 charged vacancy and defect-free calculations [4], with the

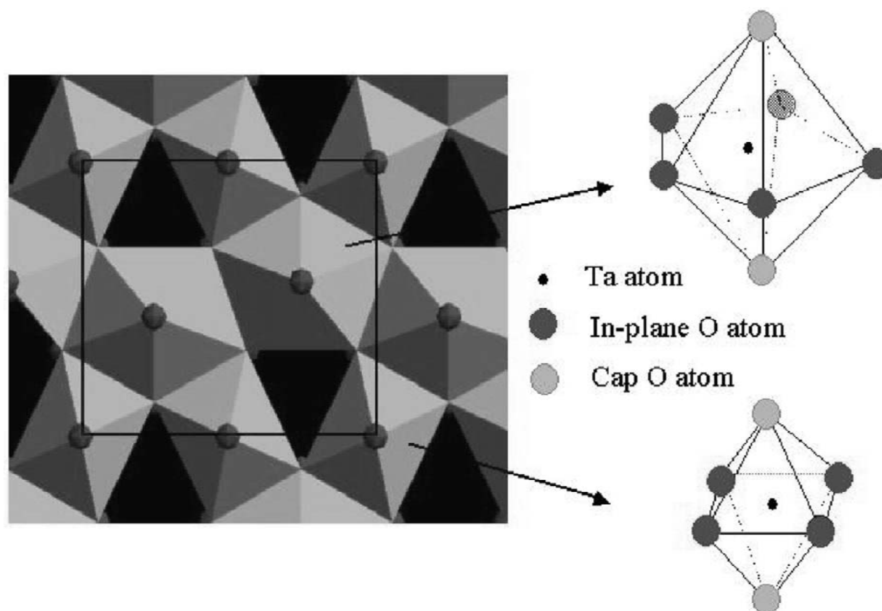

Fig. 1. Schematic of structure used in the present calculation, with the rectangle highlighting the unit cell. Also shown are the TaO_7 (top, right) and TaO_6 (bottom, right) building blocks, with the in-plane and cap site O locations explicitly identified.

defect levels scaled by the ratio of the experimental Ta_2O_5 band gap to its theoretical value. The calculated band gap of Ta_2O_5 is 2.43 eV, while the experimental value is 4.0 eV [8], and so a scaling factor of 1.65 was used. Such a discrepancy between calculated and experimental values is to be expected when the LDA is used. The stability of charged systems relative to their neutral counterparts is determined by evaluating the difference between $E(q)+\mu q$ and $E(0)$, where $E(q)$ is the total energy of a supercell with charge q, and μ is the electronic chemical potential [5]. The electronic chemical potential (close to, e.g. a metal–dielectric interface) is determined by the Fermi level (E_F) of the metal. The relative total energy of the charged vacancy supercell with respect to the corresponding neutral system is thus given as $E(q)+qE_F-E(0)$. Charged vacancy calculations were performed using the standard techniques of imposing a charge neutralizing homogeneous background charge and correcting for spurious dipole interactions [9].

3. Results and discussion

3.1. Local environment of Ta ions in Ta_2O_5

The nearest neighbor Ta–O bond lengths for the TaO_6 and TaO_7 polyhedra calculated here are in the 1.98–2.00 Å and 1.92–2.56 Å ranges, respectively, in good agreement with those observed for the actual orthorhombic crystal structure [2]. More significantly, the nearest neighbor Ta–O distances observed in amorphous Ta_2O_5 films formed under typical deposition conditions is 2.05–2.06 A, and the average coordination number (defined as the number of O atoms directly bonded to a Ta atom) of such films turns out to be in the 6.1–7.8 range [6]. Thus, the local coordination environment of Ta in the present model is consistent with that for amorphous Ta_2O_5 films, justifying the present approach for calculating properties that are largely determined by the local bonding environment.

3.2. O vacancy induced defect states

We next focus on the energetic location of defect levels created due to O vacancies. Based on the local environment, we classify O atomic (and vacancy) sites into two types as shown in Fig. 1: 'in-plane' sites, that form the base of the pentagon or the quadrilateral of the polyhedra, and 'cap' sites that cap the basal planes of the polyhedra. As we will see, these two types of vacancies display qualitatively different behavior. Lattice relaxations due to creation of in-plane type vacancies are expected to occur more easily than those due to cap type vacancies, as the in-plane O atoms are shared by three polyhedra, while the cap O atoms are shared by only two.

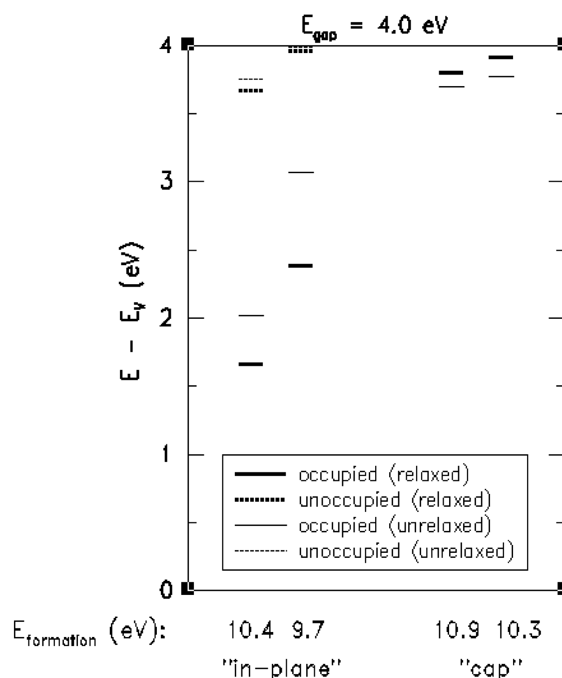

Fig. 2. Occupied and unoccupied in-plane and cap site O vacancy induced defect states, before and after lattice relaxation. Results for two vacancies of each type are shown. One of the in-plane vacancies (corresponding to the first set of states) is shared by two TaO_6 and one TaO_7 polyhedra, whereas the second in-plane vacancy (corresponding to the second set) is shared by one TaO_6 and two TaO_7 polyhedra; one of the cap site vacancies (corresponding to the third set of states) is shared by two TaO_7 polyhedra whereas the other (corresponding to the last set of states) is shared by two TaO_6 polyhedra. Vacancy formation energies calculated relative to an isolated oxygen atom in its triplet ground state are listed below the energy level diagram. All defect state energies are referenced to the top of the valence band, and shifted (as described in the text) to reflect the experimental band gap of 4.0 eV.

Creation of a neutral O vacancy in metal oxides leaves behind two electrons localized close to the vacancy location. In Ta_2O_5 (as in many other oxides [4,7]], these electrons occupy the lower of two energy states created at the band gap (the bonding orbital), with the upper state (the anti-bonding orbital) completely empty. Fig. 2 displays the occupied and unoccupied defect levels for two in-plane and two cap site vacancies, both before and after relaxation of the lattice.

The following observations can be made: (i) in-plane type vacancies result in occupied levels at the mid-gap energy range, and shallow unoccupied levels; (ii) cap type vacancies display shallow occupied states, with the unoccupied states buried in the conduction band; (iii) lattice relaxations could cause shifts of up to 0.6 eV, especially in the case of occupied levels; and (iv) vacancy formation energies (shown at the bottom of Fig. 2, and calculated using the formula: $E_{formation} = (E_{vac} + E_O) - E_{bulk}$, where E_{vac}, E_O and E_{bulk} are the total energies of the vacancy containing system, isolated oxygen atom in its triplet ground state and total energy of the defect free bulk system, respectively) of in-plane type vacancies are in general lower than those of cap type vacancies. (i) and (ii) are consistent with photoemission measurements made by Fleming et al. [8] where features in the emission spectra due to mid gap and shallow states can be clearly seen.

3.3. Relative stability of charged vacancies

The stability of a charge state of a vacancy is determined by the position of the vacancy induced defect levels with respect to the local chemical potential. For vacancies close to the metal–insulator interface, the local chemical potential is largely determined by the metal Fermi level. Fig. 3 displays the relative total energies of in-plane and cap type vacancies in various charge states as a function of the local chemical potential or Fermi energy (E_F), defined with respect to the valence band minimum of Ta_2O_5 (E_V). The lattice structure at each charge state was completely relaxed. In each case, the total energy is referenced to that of the neutral vacancy.

Let us consider Fig. 3a. For very low values of the local Fermi energy, the +2 charged state of the vacancy is predicted to be most stable, and for

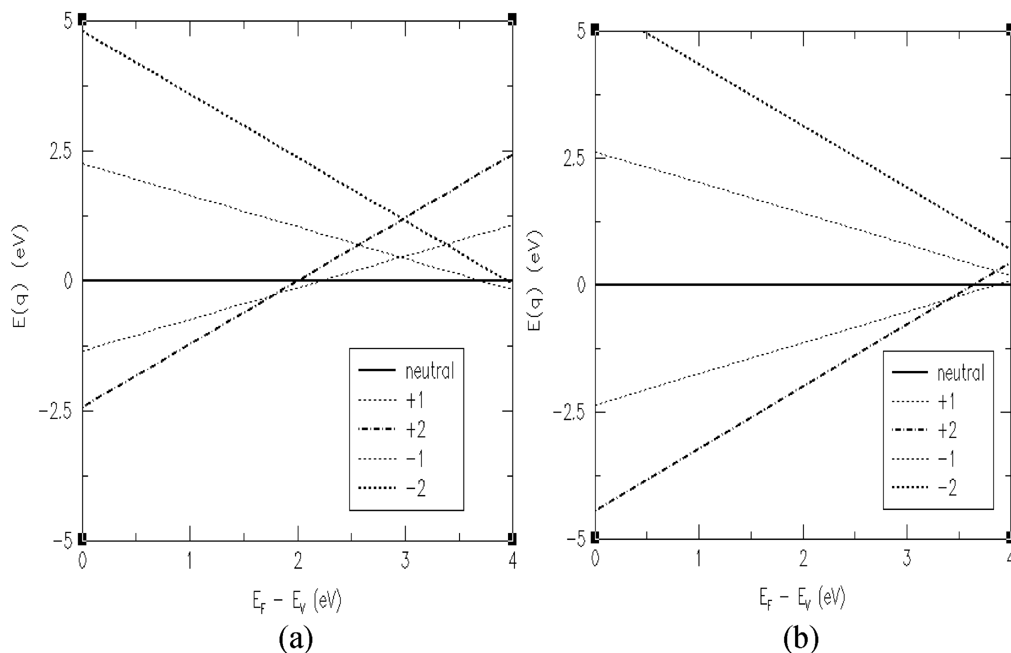

Fig. 3. Relative total energy $E(q)$ of in-plane (a) and cap (b) type vacancies as a function of the chemical potential (which is here assumed to be the Fermi energy); q denotes the charge state of the vacancy ($q = +2$, $+1$, 0, -1, or -2).

medium to high values of $E_F - E_V$, the neutral state is seen to be most stable. These predictions are consistent with the location of the occupied state at the mid gap energy range, and the unoccupied state close to the conduction band maximum in the case of in-plane type vacancies: clearly, when $E_F - E_V$ is very low, the two electrons from the occupied state will tend to be transferred to the Fermi level (making the +2 state more stable), while no transfer of charge will occur for most other values of $E_F - E_V$ making the neutral state most stable. Thus, barring the small $E_F - E_V$ ranges at which the +1 and −1 charge states are stable, the +2 and neutral states are seen to be the most stable for a wide range of $E_F - E_V$. Similar arguments hold for the cap site vacancy (Fig. 3b), for which the +2 charged state is most stable for a wide range of local Fermi energies.

4. Summary

Density functional calculations were performed in order to characterize O vacancy defects in Ta_2O_5. A simplified version of the crystalline orthorhombic phase of Ta_2O_5 was used in this study. The local coordination environment of the present model was found to be similar to that of Ta_2O_5 films. Results indicate that O vacancies in Ta_2O_5 can be broadly classified into 'in-plane' and 'cap' types, based on their location in the lattice. The 'in-plane' type vacancies display deep or mid gap level occupied states, and shallow unoccupied states, while the 'cap' type vacancies result in shallow occupied states. For a wide range of local Fermi level or chemical potential, the neutral and +2 charged states of the in-plane type vacancy and the +2 charge state of the cap type vacancy are most stable.

References

[1] C. Chaneliere, J.L. Autran, R.A.B. Devine, B. Balland, Mater. Sci. Eng. R22 (1998) 269.

[2] N.C. Stephenson, R.S. Roth, Acta Crystallogr. B27 (1971) 1037.

[3] G. Kresse, J. Hafner, Phys. Rev. B 47 (1993) 558;
G. Kresse, J. Hafner, Phys. Rev. B 54 (1996) 11169.

[4] A.S. Foster, V.B. Sulimov, F. Lopez Gejo, A.L. Shluger, R.M. Nieminen, Phys. Rev. B 64 (2001) 224108.

[5] A. Yokozawa, Y. Miyamoto, Phys. Rev. B 55 (1997) 13783.

[6] H. Kimura, J. Mizuki, S. Kamiyama, H. Suzuki, Appl. Phys. Lett. 66 (1995) 2209.

[7] A.S. Foster, F. Lopez Gejo, A.L. Shluger, R.M. Nieminen, Phys. Rev. B 65 (2002) 174117.

[8] R.M. Fleming et al., J. Appl. Phys. 88 (2000) 850.

[9] See the VASP manual at http://cms.mpi.univie.ac.at/vasp/vasp/vasp.html;
Also see G. Makov, M.C. Payne, Phys. Rev. B 51 (1995) 4014.